Diagnostic Accuracy Study

Medicine®

OPEN

Improved differentiation between high- and low-grade gliomas by combining dual-energy CT analysis and perfusion CT

Yoko Kaichi, MD[a,*], Fuminari Tatsugami, MD[a], Yuko Nakamura, MD[a], Yasutaka Baba, MD[a], Makoto Iida, MD[a], Toru Higaki, PhD[a], Masao Kiguchi, RT[b], So Tsushima, MSc[c], Fumiyuki Yamasaki, MD[d], Vishwa Jeet Amatya, MD[e], Yukio Takeshima, MD[e], Kaoru Kurisu, MD[d], Kazuo Awai, MD[a]

Abstract

The purpose of this study was to investigate the value of the cerebral blood volume (CBV) obtained with perfusion computed tomography (CT) and the electron density (ED) measured by dual-energy CT for differentiating high- from low-grade glioma (HGG, LGG).

The CBV and ED were obtained in 9 LGG and 7 HGG patients. The CBV and ED of LGGs and HGGs were compared. Receiver operating characteristic (ROC) curves were generated for CBV, ED, and CBV plus ED. The correlation between CBV, ED, and the MIB-1 labeling index of the tumors was examined. All of these analyses were also performed using relative CBV (rCBV) and ED (rED) (the value of tumors/the value of contralateral white matter).

The mean CBV, ED, rCBV, and rED values were significantly higher in HGG than LGG ($P < .05$). By ROC analysis, the combination of rCBV plus rED as well as CBV plus ED were more accurate than CBV, ED, rCBV, rED alone. There was a significant correlation between ED and MIB-1 ($P = .04$).

ED improved diagnostic accuracy of perfusion CT for differentiating HGG from LGG.

Abbreviations: ADC = apparent diffusion coefficient, AUC = area under the curve, CBV = cerebral blood volume, CT = computed tomography, CT_{DI} = CT dose index, DECT = dual-energy CT, ED = electron density, FLAIR = fluid-attenuated inversion recovery, HGG = high-grade glioma, LGG = low-grade glioma, MRI = magnetic resonance imaging, NPV = negative predictive value, PCT = perfusion CT, PPV = positive predictive value, rCBV = relative CBV, rED = relative ED, ROC = receiver operating characteristic, ROIs= regions of interests, T1WI = T1-weighed image, T2WI = T2-weighed image, WHO = World Health Organization.

Keywords: cerebral blood volume, dual-energy CT, electron density, glioma, perfusion CT

1. Introduction

The treatment and prognosis of cerebral gliomas depend on the histological tumor grade. Quantification of tumor angiogenesis and cell density is important for predicting the tumor grade. However, computed tomography (CT) and magnetic resonance imaging (MRI) findings obtained by conventional techniques may not accurately predict the histological glioma grade.[1,2] The diffusion-weighted imaging derived apparent diffusion coefficient (ADC) measures the average diffusion of water molecules within each voxel. Although the ADC has been shown to decrease in the presence of hypercellularity, some debate remains as to whether it is predictive of the tumor grade.[3–7]

The cerebral blood volume (CBV), defined as the volume of blood flowing in blood vessels per 100 g of brain tissue at a particular point in time, can be used to quantify microvascular density.[8–11] Perfusion CT (PCT) is a reliable technique for the quantification of CBV in a single acquisition with a single bolus of contrast medium.[12] Perfusion studies have been used to differentiate high- from low-grade gliomas (HGG and LGG).[1,10,11,13–15] However, radiation exposure of the normal brain and eyes limits its clinical use, especially in the young and in patients with low-grade tumors.

Dual-energy CT (DECT) can measure the electron density (ED) of substances[16–19]; the subject is scanned at 2 different energies (tube voltages). The ED reflects the probability of an electron being present at a specific location; it depends on the kind of molecule and the molecular structure,[20] and it can be determined with high accuracy using a 2-rotation kV-mA switching DECT system.[19]

Although MRI is the gold standard in neuro-oncology, some patients may not be able to receive MRI due to pacemakers or claustrophobia. On the other hand, CT is more widely available and the only technique in the ED or overnight in some hospitals. To the best of our knowledge, ED in gliomas measured by DECT has neither been reported, nor has the correlation between ED and the histological glioma grade. The purpose of this study was to compare the accuracy of CBV obtained from PCT scans and

Editor: Rimas Vincas Lukas.

Dr Awai reports grants from Toshiba Medical Systems.

The authors have no conflicts of interest to disclose.

[a] Diagnostic Radiology, [b] Department of Radiology, Hiroshima University, Minami-ku, Hiroshima, [c] Canon Medical Systems Corporation, Otawara, Tochigi, [d] Department of Neurosurgery, Graduate School of Biomedical Sciences, [e] Department of Pathology, Institute of Biomedical and Health Sciences, Hiroshima University, Minami-ku, Hiroshima, Japan.

[*] Correspondence: Yoko Kaichi, Diagnostic Radiology, Hiroshima University, Kasumi 1-2-3, Minami-ku, Hiroshima 734-8551, Japan (e-mail: kaichi@hiroshima-u.ac.jp).

Medicine (2018) 97:32(e11670)

Received: 1 October 2017 / Accepted: 3 July 2018

http://dx.doi.org/10.1097/MD.0000000000011670

ED measured on DECT images for differentiating HGG from LGG. We also assessed whether the CBV plus ED improve diagnostic accuracy.

2. Materials and methods

2.1. Patients

This retrospective study was approved by our institutional review board; patient informed consent was waived. Using entries in our radiological database made between April 2014 and August 2016, we reviewed 84 patients with intracranial lesions who had undergone PCT and DECT. In our institution, except for patients under 20-year-old, routine imaging examination includes head CT containing PCT and DECT as well as conventional MRI when the brain tumors are detected and seemed to require biopsy or surgery. Of the 84 patients, we enrolled 21 with a pathological diagnosis of cerebral glioma; 5 patients were subsequently excluded because they had received surgery, radiation therapy, or chemotherapy. Consequently, 16 cerebral glioma patients (9 men, 7 women; median age 60.5 ± 16.3 (standard deviation [SD]) years) who had not undergone any kind of treatment or biopsy at the time of CT examination were enrolled.

2.2. CT acquisition

2.2.1. Dual-energy CT. Noncontrast CT scans of the head were obtained on a 320-detector CT scanner (Aquilion ONE; Toshiba Medical Systems Corp., Tokyo, Japan) in dual-energy mode with a 2-rotation kV-mA switching system. DECT scans were performed at tube voltages of 80 kV (570 mA) and 135 kV (100 mA) using the volume scanning method. The time for switching the tube voltage between 80 and 135 kV was 0.4 seconds. The other scanning parameters were rotation time, 0.5 seconds and z-coverage 80 to 128 mm including the entire tumor. All images were reconstructed with filtered back projection; the slice thickness and reconstruction interval were 0.5 mm. The CT dose index (CT_{DI}) displayed on the CT scanner was recorded for each patient.

2.2.2. Perfusion CT. DECT was followed by PCT. Using a dual-shot injector (Nemoto Kyorindo, Tokyo, Japan), we delivered 32 mL of nonionic contrast material (iopamidol, Oiparomin 370 mg I/mL; Fuji Pharmaceutical Co., Toyama, Japan) at a rate of 4 mL/s to all patients. This was followed by 25 mL of a 0.9% saline solution injected at the same flow rate as the contrast material. PCT scanning began 5 seconds after the start of contrast material injection. The scan parameters were collimation, 320×0.5 mm; rotation time, 1.0 seconds; tube voltage, 80 kV; tube current, 100 mA. The scan range (z-coverage, 75–110 mm) included the entire target tumor. CT scans were performed every 2 seconds for 35 seconds, then every 5 seconds for 20 seconds; 20 series of volume data were obtained. All images were reconstructed with adaptive iterative dose reduction 3D at the standard setting; the slice thickness and reconstruction interval were 0.5 mm. Reconstructed image data were transferred to a workstation (AZE VirtualPlace Fujin Rajin 350 version 3.5008; AZE Ltd., Tokyo, Japan) for postprocessing. The displayed CT_{DI} was recorded for each patient.

2.3. MR acquisition

For all patients, conventional MRI including T1-weighed image (T1WI), T2-weighed image (T2WI), fluid-attenuated inversion recovery (FLAIR), diffusion-weighted image, and postcontrast T1WI were obtained by using a 3T magnetic resonance (MR) system (Signa HDxt, GE Healthcare, Milwaukee, WI) using an 8-channel phased-array head coil (USA Instruments, Aurora, OH). The following imaging parameters were used: T1WI: TR/TE 400/17.0 milliseconds; T2WI: TR/TE 4500/99.7 milliseconds; FLAIR: TR/TE/TI 10002/145.9/2400 milliseconds; postcontrast T1WI: TR/TE 400/17.0 milliseconds. Postcontrast images were obtained after intravenous administration of gadopentetate dimeglumine (0.1 mmol/kg, Magnevist; Bayer Vital GmbH, Leverkusen, Germany) or gadobutrol (0.1 mmol/kg, Gadovist; Bayer). Field of view (FOV) of 220×220 mm was applied to all images.

2.4. Histopathological evaluations

The median interval between the acquisition of CT studies and stereotactic biopsy or surgery for evaluation of the tumor histopathology was 6 days (range 2–109 days) in the 16 patients. All histopathological specimens were examined by a neuropathologist and were graded according to the 2007 World Health Organization (WHO) guidelines[21]; characterization of HGG and LGG were determined based on cellularity, pleomorphism, nuclear atypia, mitotic activity, and vascular proliferation of the tumor. According to their degree of malignancy, they were classified as low-grade (I or II) or high-grade (III or IV) gliomas. The MIB-1 labeling index, which is closely related to the histological glioma grade,[22] was recorded in all patients. The MIB-1 labeling index was measured in the microscopic area that showed the greatest number of immunopositive nuclei.

2.5. Methods of evaluation

For dual-energy analysis, we used raw data-based analysis. ED maps were automatically created on the CT console. Perfusion CBV maps were generated on a different workstation with PCT software; a 2-compartment model and a deconvolution method were used. The superior sagittal sinus was applied as the venous output function and the largest and most proximal artery observed at the imaging level as the arterial input function.

One board-certified radiologist with 11 years of experience in neuro-radiology who was blinded to clinical information and pathology results, identified brain tumors by reference to the findings on MRI and placed multiple regions of interests (ROIs) in tumor areas with the highest CBV value and chose the maximum value among the multiple ROIs (Fig. 1A); the highest value was presumed to represent the most malignant part of the tumor.[23] The ROIs were placed in the solid portion of the tumors, avoiding necrotic areas and cystic degeneration. The mean CBV value of contralateral white matter was adopted as a reference of relative perfusion. ED map were reformatted to the same slices with CBV map, and ROIs were placed at identical sites on the ED map and on PCT scans (Fig. 1B). We also calculated the relative CBV (rCBV) and ED (rED) (the value of tumors/the value of contralateral white matter).

2.6. Statistical analysis

Two-sample *t* tests were used to compare CBV and ED between LGGs and HGGs. The sensitivity, specificity, and the positive and negative predictive value (PPV, NPV) of the CBV, ED, and CBV plus ED for the diagnosis of LGG and HGG were calculated. The diagnostic accuracy of these factors was assessed with receiver operating characteristic (ROC) analysis and the area under the curve (AUC) for each parameter was calculated. Optimal cut-off values for classifying the tumors as low- or high-grade were

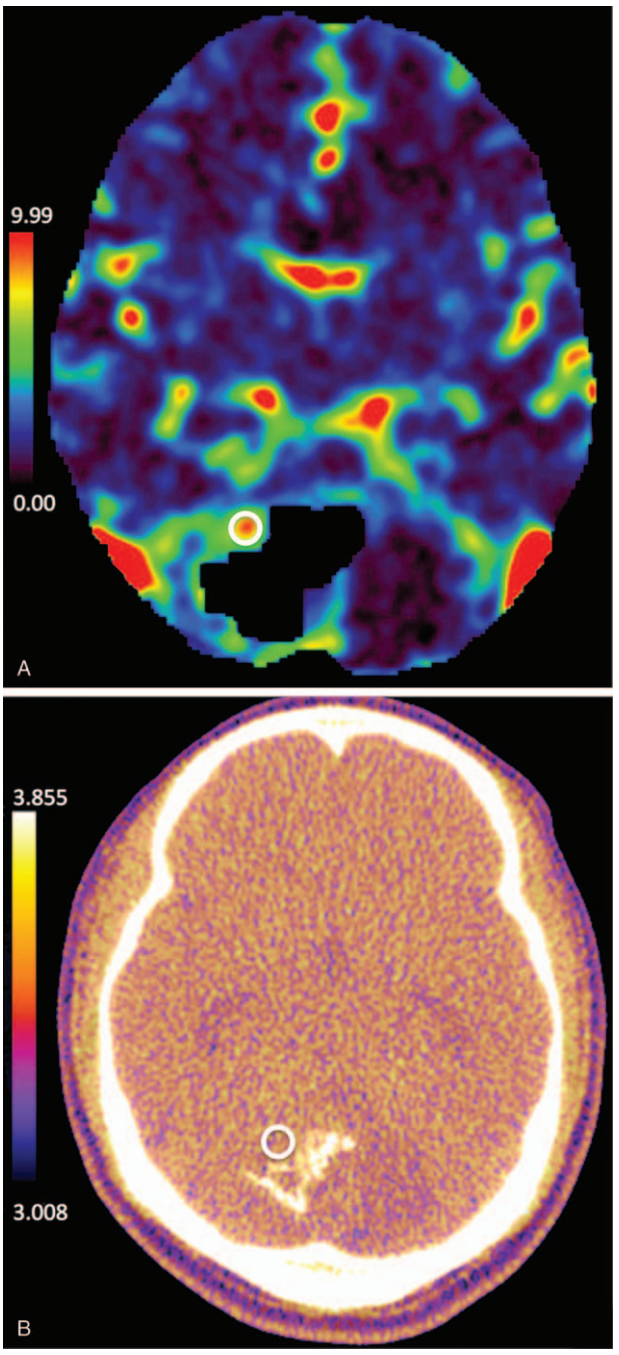

Figure 1. A 20-year-old man with pilocytic astrocytoma. Regions of interest (ovals) were placed in areas of the tumor with the highest cerebral blood volume. (A) Cerebral blood volume map: measured value 9.14 mL/100 g. (B) Electron density map: measured value 3.44×10^{23}/mL.

determined according to the Youden criterion; it marks the point on an ROC curve where "sensitivity + specificity − 1" is maximal. The correlation between MIB-1 and CBV and between MIB-1 and ED was examined with the Pearson correlation coefficient. All of these analyses were also performed using rCBF and rED. Values of $P < .05$ were considered statistically significant.

3. Results

Of the 16 patients, 9 harbored LGGs (pilocytic [n = 2] and diffuse [n = 4] astrocytomas; oligodendrogliomas [n = 3]; 5 men, 4 women); all 7 HGGs were glioblastomas (4 men, 3 women). The median CT_{DI} for DECT was 33.1 mGy (range 30.1–36.2 mGy); for PCT, it was 103.3 mGy (range 94.9–106.1 mGy).

Table 1

Cerebral blood volume and electron density for gliomas.

	Low-grade glioma	High-grade glioma	*P* value
No. of patients	9	7	
CBV, mL/100 g	4.20 ± 2.55	7.28 ± 3.33	.02
ED, $\times 10^{23}$/mL	3.41 ± 0.03	3.45 ± 0.02	.02
rCBV	2.16 ± 1.13	4.25 ± 1.38	< .01
rED, $\times 10^{-1}$	9.94 ± 0.08	10.02 ± 0.05	.04

All variables except the number of patients are presented as the mean ± standard deviation. CBV = cerebral blood volume, ED = electron density, rCBV = relative CBV, rED = relative ED.

As shown in Table 1, the mean CBV and ED values were significantly higher in HGGs than LGGs (both, $P = .02$), although there was some overlapping (Fig. 2A and B). The mean rCBV and rED values were also significantly higher in HGGs than LGGs (rCBV, $P < .01$; rED, $P = .04$) (Fig. 2C and D). The parameter consisting of the combination of CBV plus ED was significantly different between LGG and HGG ($P = .01$). The parameter consisting of the combination of rCBV plus rED was also significantly different between LGG and HGG ($P < .01$). Table 2 shows cut-off values of these parameters: sensitivity, specificity, PPV, and NPV.

Figure 3 shows ROC curves. CBV plus ED (AUC = 0.90) had higher accuracy for differentiating HGG from LGG than CBV alone and ED alone (both, AUC = 0.86) (Fig. 3A–C). ROC analysis showed that rCBV plus rED (AUC = 0.92) also had higher accuracy than rCBV alone (AUC = 0.89) and rED alone (AUC = 0.78) (Fig. 3D–F).

There was a statistically significant correlation between ED and MIB-1 ($r = 0.51$, $P = .04$) but not between CBV and MIB-1 ($r = 0.33$, $P = .22$) (Fig. 4A and B). There was no significant correlation between rED and MIB-1 ($r = 0.38$, $P = .15$) nor between rCBV and MIB-1 ($r = 0.34$, $P = .20$) (Fig. 4C and D).

4. Discussion

We first document the usefulness of the ED obtained from DECT scans for differentiating HGG from LGG. We also show that in combination, the rCBV and rED values as well as CBV and ED values yielded higher diagnostic accuracy than CBV, ED, rCBV, rED alone and that ED correlated with the MIB-1 labeling index. We calculated ratios as well as absolute values, which might help in the generalization of results, and use of their data by other groups with different equipment. There is a significant difference in CBV, rCBV, ED, and rED between LGGs and HGGs. There is also a significant correlation between ED and MIB-1, which would support the value of ED.

Various MRI techniques including conventional MRI, MR spectroscopy, and MR perfusion have been used for grading glioma. Though conventional MRI provides important anatomical findings, it is insufficient in grading gliomas. Previous studies reported that conventional MRI showed sensitivity in identifying HGGs ranging from 55.1% to 85.7%[14,15,24–27] and rCBV measurements improved grading gliomas.[14,24,28,29] MR spectroscopy may also provide important supplemental information to that of conventional MR imaging, although it alone has not been shown to be reliable in grading gliomas.[14,30–32] PCT has advantages over MR perfusion because of easy accessibility and postprocessing. MR perfusion techniques have some limitations

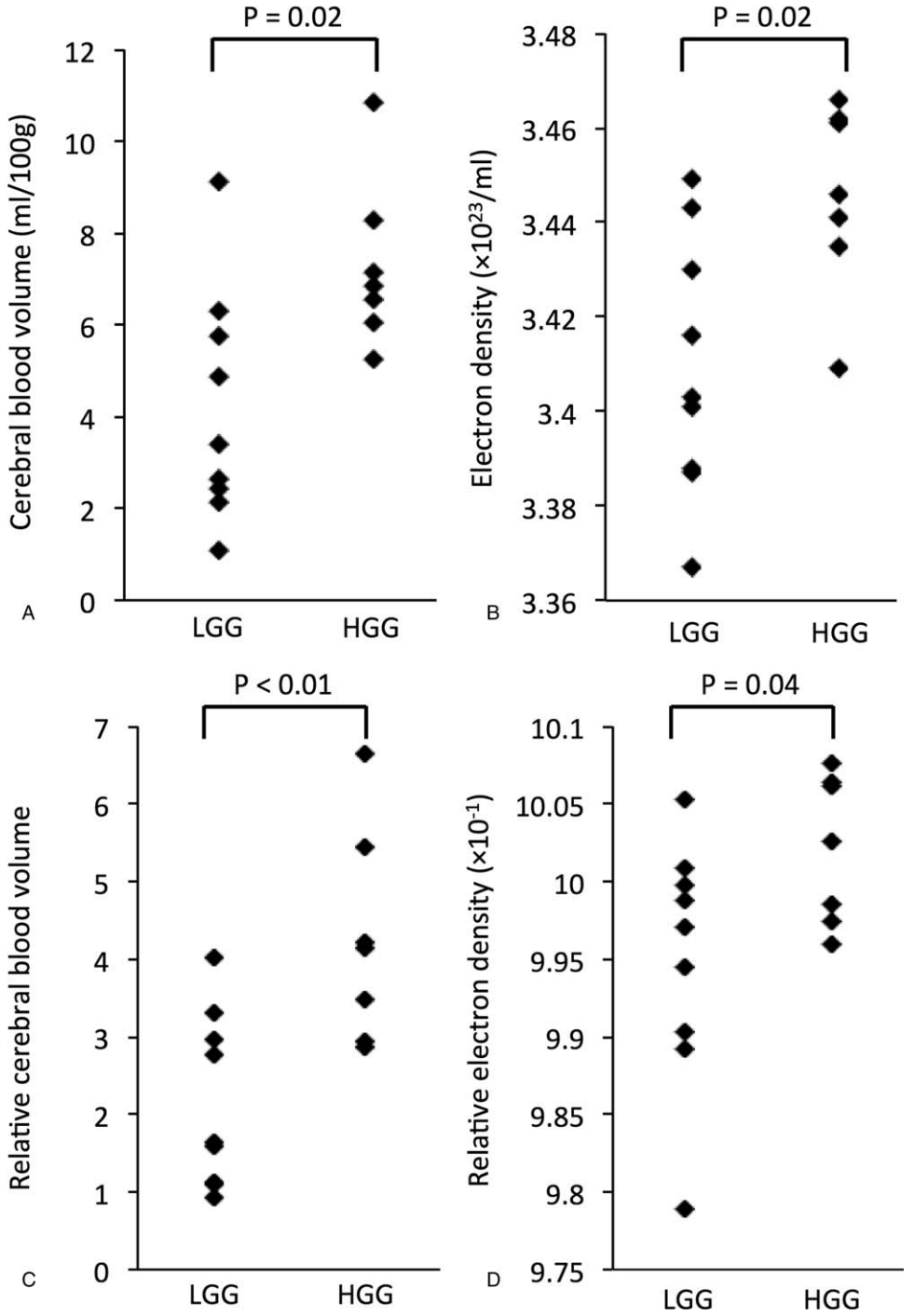

Figure 2. Scatter diagram shows cerebral blood volume (CBV) (A), electron density (ED) (B), relative CBV (rCBV) (C), and relative ED (rED) values (D) for low- and high-grade gliomas (LGG, HGG). The mean CBV, ED, rCBV, and rED values were significantly higher for HGG than LGG ($P < .05$).

including sensitivity to the magnetic field inhomogeneities due to hemorrhagic products in gliomas and higher cost of imaging hardware compared to CT. However, limitations of PCT generally include the radiation dose involved with the procedure. MR and CT should be treated complementarily for grading gliomas.

The degree of microvascular proliferation is one of the most important features in grading glioma; the other factors are nuclear atypia, mitoses, and necrosis.[33] Thus, imaging techniques that yield hemodynamic information about the tumors may help in their characterization.[8–11,34] In HGGs, rapid cell growth demands activating metabolism and causes cellular hypoglycemia and hypoxia, which lead to the production of angiogenic cytokines. Consequently, neoangiogenesis occurs[35] and increased capillary attenuation leads to higher blood volume and blood flow in the tumor bed.[35,36] HGG is also characterized by high density of tumor cells and high nucleocytoplasmic ratio.[37,38] In molecules, areas of ED are tend to be found around the atom and its bonds.[39] In conjugated systems such as nucleic acid, ED may be higher than in single-bond systems

Table 2

The diagnostic accuracy of CBV, ED, rCBV, and rED for differentiating high-grade glioma from low-grade glioma.

	Cut-off value	Sensitivity	Specificity	PPV	NPV
CBV, mL/100 g	5.26	100	67	70	100
ED, $\times 10^{23}$/mL	3.44	85	78	75	88
rCBV	2.88	100	67	70	100
rED, $\times 10^{-1}$	10.02	57	90	80	73
CBV plus ED	0.364	100	78	78	100
rCBV plus rED	0.778	100	78	78	100

All parameters except cut-off value are presented as percent.

CBV = cerebral blood volume, ED = electron density, NPV = negative predictive value, PPV = positive predictive value, rCBV = relative CBV, rED = relative ED.

because of the short bond distance.[40] Therefore, the ED, which can be analyzed without requiring contrast media or irradiation, may reflect the cell density and the nucleocytoplasmic ratio and it was as accurate as the CBV for differentiating HGG from LGG. CBV and ED may be complementary parameter; however, they may correlate to each other because both of them reflect tumor growth.

On raw data-based DECT images, beam-hardening artifacts are lower than on image-based DECT images[41,42]; this helps to improve the accuracy of ED maps. Commercially available DECT imaging systems feature 2-rotation kV-mA switching; 1 scan rotation is at high- and the other at low-tube voltage. This ensures complete energy separation between the high- and low-tube voltage scans and makes possible highly accurate dual-

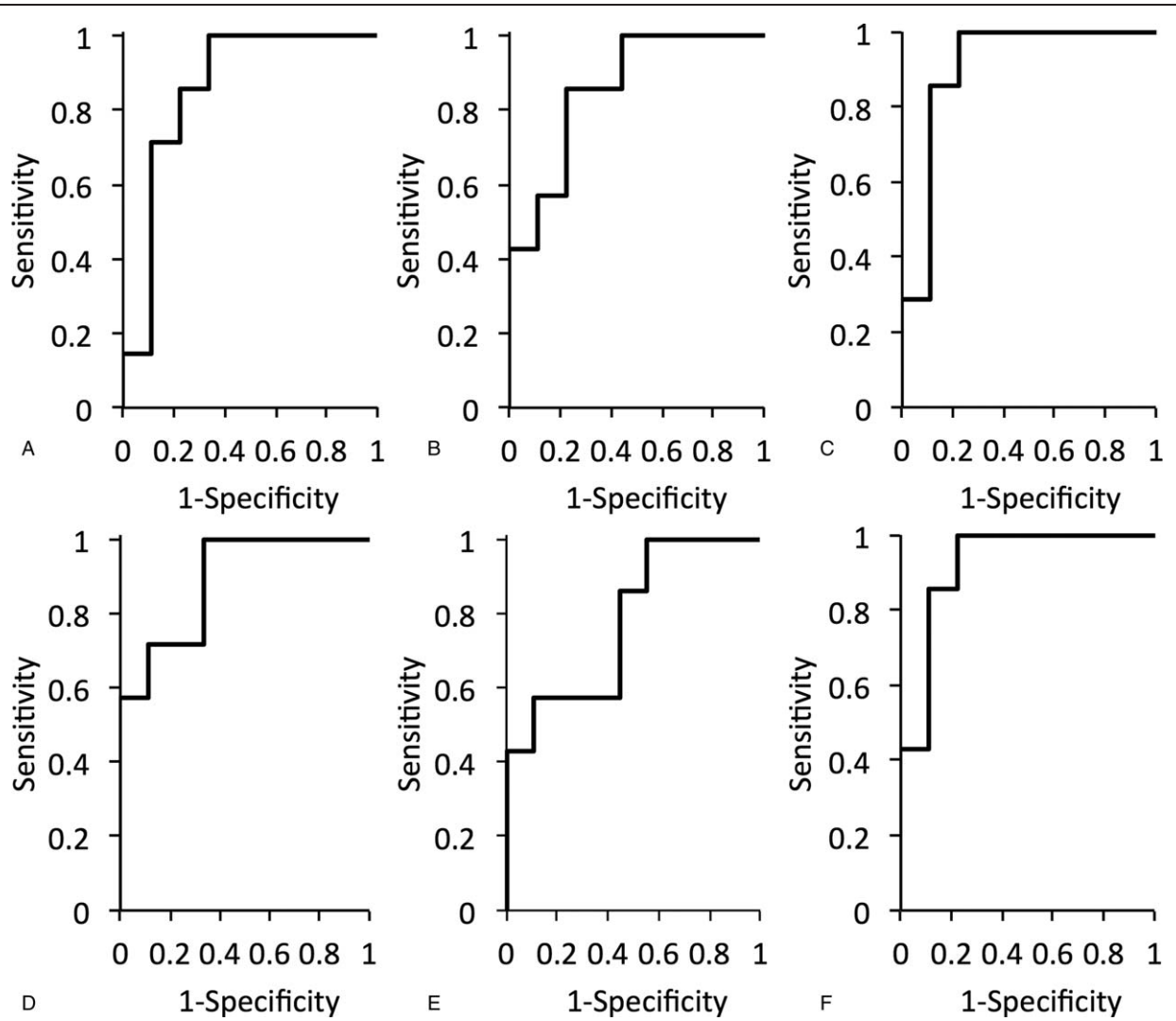

Figure 3. Graphs show areas under ROC curves. The AUC values for the cerebral blood volume (CBV), electron density (ED), and CBV plus ED were 0.86, 0.86, and 0.90, respectively. The AUC values for the rCBV, rED, and rCBV plus rED were 0.89, 0.78, and 0.92, respectively. AUC = area under the curve, ROC = receiver operating characteristic.

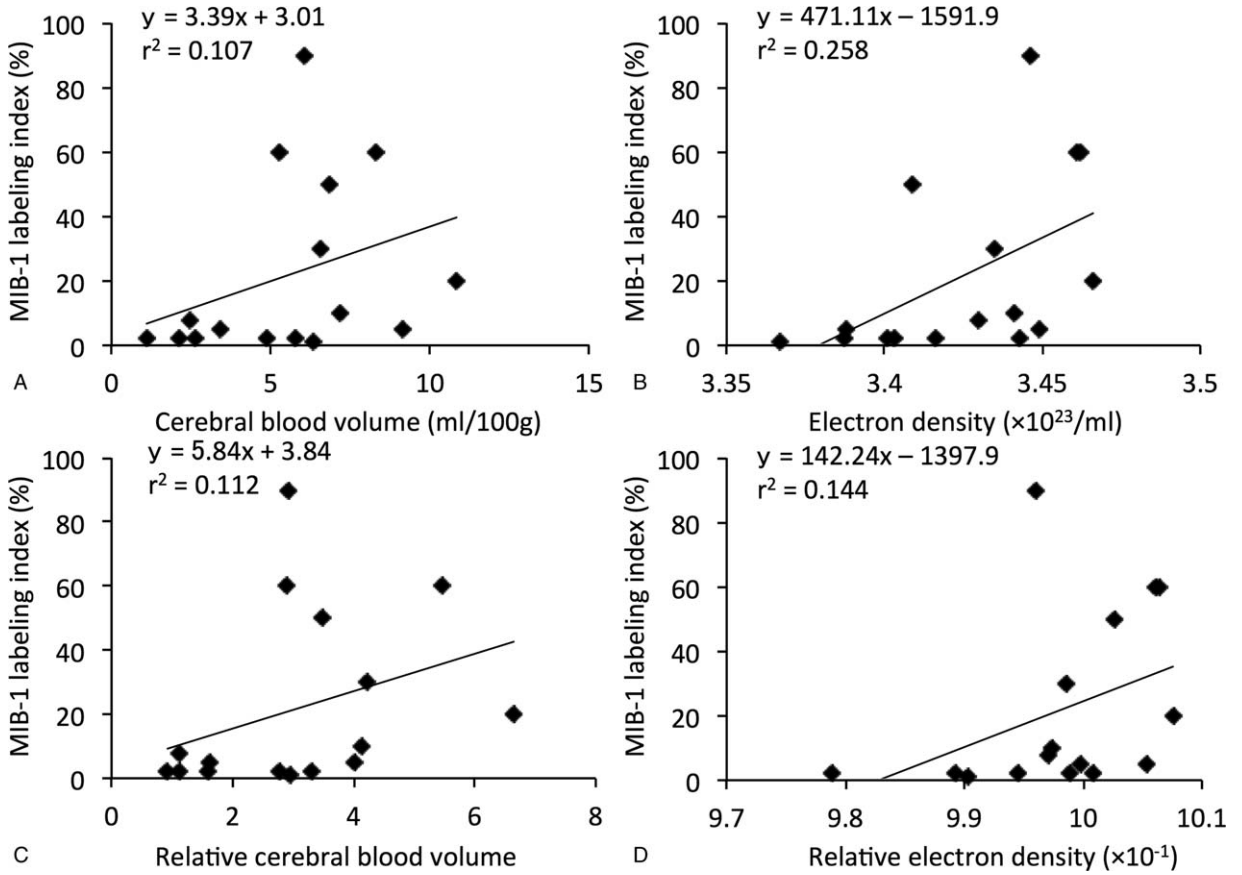

Figure 4. Scatter diagram showing the correlation between the cerebral blood volume (CBV) and the MIB-1 labeling index (A), between electron density (ED) and the MIB-1 labeling index (B), between relative CBV (rCBV) and MIB-1 labeling index (C), and between relative ED (rED) and MIB-1 labeling index (D). Correlation analysis revealed a significant correlation between electron density and the MIB-1 labeling index ($r = 0.51$, $P = .04$). There was no statistically significant correlation between CBV and MIB-1 ($r = 0.40$, $P = .12$), between rED and MIB-1 ($r = 0.38$, $P = .15$), and between rCBV and MIB-1 ($r = 0.34$, $P = .20$).

energy analyses.[42–44] Tatsugami et al[19] reported that ED could be determined with mean errors of 1.3% (SD 1.5%) using a 2-rotation kV-mA switching DECT system and the raw data-based method.

In this study, the estimated CT_{DI} associated with the dual-energy mode for estimating ED was 33.1 mGy, and thus much lower than for PCT (103.3 mGy) and lower than the diagnostic reference level for head CT recommended by J-RIME report (85 mGy)[45] or the International Commission on Radiological Protection (60 mGy).[46] Therefore, ED measurements can be obtained easily in young patients and patients with low-grade tumors.

Importantly, we identified the value of the combination of CBV, reflecting the vascular density, plus the ED, reflective of the cell density and nucleocytoplasmic ratio, for differentiating HGG from LGG. As the malignancy of gliomas depends on both increased microvascular density and cell proliferation, knowledge of the ED may help to overcome some of the diagnostic limitations of conventional and perfusion imaging.

Given the positive correlation we identified between ED and MIB-1, the former may serve as an indicator of cell proliferation. It may be possible to determine the degree of malignancy without the use of contrast media because the ED can be determined on plain DECT scans.

This study has some limitations. First, we do not have genomic data in our patient population, although WHO is moving away from histological grading and toward genomic markers. However, histological grading well corresponds genomic one and our findings would apply to the 2016 WHO classification.[47] Second, the histologic specimens might not have corresponded with the areas of our CBV and ED measurements. Third, the presence of oligodendrogliomas and pilocytic astrocytomas among the LGGs may have given rise to selection bias because in these tumors, CBV is higher than in astrocytomas.[48,49] Finally, the small number of glioma patients limits the statistical inference and the conclusion that can be drawn from our results. Although those are preliminary results, ED can be obtained with no extra radiation dose and no contrast media, and a larger study population is needed to confirm our preliminary findings. At last, it is uncertain whether our combination method is applicable to diagnosing other brain tumors.

In conclusion, the ED obtained by DECT with a raw data-based method contributed to differentiating HGG from LGG. Our findings also suggest that for a diagnosis, the combination of rCBV plus rED as well as CBV plus ED was superior to the use of CBV, ED, rCBV, rED alone. There was a significant correlation between ED and MIB-1, which would support the value of ED. ED measurements may be of additive diagnostic value and may impact the initial management of patients with gliomas.

Author contributions

Conceptualization: Yoko Kaichi.

Data curation: Yoko Kaichi, Yuko Nakamura, Yasutaka Baba, Makoto Iida, Toru Higaki, Masao Kiguchi, Fumiyuki Yamasaki.
Investigation: Fumiyuki Yamasaki.
Methodology: Masao Kiguchi, So Tsushima, Vishwa Jeet Amatya, Yukio Takeshima.
Software: Toru Higaki, So Tsushima.
Validation: Vishwa Jeet Amatya, Yukio Takeshima.
Writing – original draft: Yoko Kaichi.
Writing – review and editing: Fuminari Tatsugami, Kaoru Kurisu, Kazuo Awai.

References

[1] Law M, Yang S, Babb JS, et al. Comparison of cerebral blood volume and vascular permeability from dynamic susceptibility contrast-enhanced perfusion MR imaging with glioma grade. AJNR Am J Neuroradiol 2004;25:746–55.
[2] Law M, Cha S, Knopp EA, et al. High-grade gliomas and solitary metastases: differentiation by using perfusion and proton spectroscopic MR imaging. Radiology 2002;222:715–21.
[3] Sugahara T, Korogi Y, Kochi M, et al. Usefulness of diffusion-weighted MRI with echo-planar technique in the evaluation of cellularity in gliomas. J Magn Reson Imaging 1999;9:53–60.
[4] Hayashida Y, Hirai T, Morishita S, et al. Diffusion-weighted imaging of metastatic brain tumors: comparison with histologic type and tumor cellularity. AJNR Am J Neuroradiol 2006;27:1419–25.
[5] Kono K, Inoue Y, Nakayama K, et al. The role of diffusion-weighted imaging in patients with brain tumors. AJNR Am J Neuroradiol 2001; 22:1081–8.
[6] Castillo M, Smith JK, Kwock L, et al. Apparent diffusion coefficients in the evaluation of high-grade cerebral gliomas. AJNR Am J Neuroradiol 2001;22:60–4.
[7] Lam WW, Poon WS, Metreweli C. Diffusion MR imaging in glioma: does it have any role in the pre-operation determination of grading of glioma? Clin Radiol 2002;57:219–25.
[8] Wong JC, Provenzale JM, Petrella JR. Perfusion MR imaging of brain neoplasms. AJR 2000;174:1147–57.
[9] Shin JH, Lee HK, Kwun BD, et al. Using relative cerebral blood flow and volume to evaluate the histopathologic grade of cerebral gliomas: preliminary results. AJR 2002;179:783–9.
[10] Ding B, Ling HW, Chen KM, et al. Comparison of cerebral blood volume and permeability in preoperative grading of intracranial glioma using CT perfusion imaging. Neuroradiology 2006;48:773–81.
[11] Jain R, Ellika SK, Scarpace L, et al. Quantitative estimation of permeability surface-area product in astroglial brain tumors using perfusion CT and correlation with histopathologic grade. AJNR Am J Neuroradiol 2008;29:694–700.
[12] Miles KA, Charnsangavej C, Lee FT, et al. Application of CT in the investigation of angiogenesis in oncology. Acad Radiol 2000;7:840–50.
[13] Lev MH, Rosen BR. Clinical applications of intracranial perfusion MR imaging. Neuroimaging Clin N Am 1999;9:309–31.
[14] Law M, Yang S, Wang H, et al. Glioma grading: specificity and predictive values of perfusion MR imaging and proton MR spectroscopic imaging compared with conventional MR imaging. AJNR 2003;24:1989–98.
[15] Ellika SK, Jain R, Patel SC, et al. Role of perfusion CT in glioma grading and comparison with conventional MR imaging features. AJNR 2007;28:1981–7.
[16] Landry G, Reniers B, Granton PV, et al. Extracting atomic numbers and electron densities from a dual source dual energy CT scanner: experiments and a simulation model. Radiother Oncol 2011;100:375–9.
[17] Van Abbema JK, Van der Schaaf A, Kristanto W, et al. Feasibility and accuracy of tissue characterization with dual source computed tomography. Phys Med 2012;28:25–32.
[18] Saito M. Potential of dual-energy subtraction for converting CT numbers to electron density based on a single linear relationship. Med Phys 2012;39:2021–30.
[19] Tatsugami F, Higaki T, Kiguchi M, et al. Measurement of electron density and effective atomic number by dual-energy scan using a 320-detector computed tomography scanner with raw data-based analysis: a phantom study. J Comput Assist Tomogr 2014;38:824–7.
[20] Domingo LR. Molecular electron density theory: a modern view of reactivity in organic chemistry. Molecules 2016;21:E1319.
[21] Louis DN, Ohgaki H, Wiestler OD, et al. WHO Classification of Tumours of the Central Nervous System. IARC, Lyon:2007.
[22] Burger PC, Shibata T, Kleihues P. The use of the monoclonal antibody Ki-67 in the identification of proliferating cells: application to surgical neuropathology. Am J Surg Pathol 1986;10:611–7.
[23] Wolf RL, Wang J, Wang S, et al. Grading of CNS neoplasms using continuous arterial spin labeled perfusion MR imaging at 3 Tesla. J Magn Reson Imaging 2005;22:475–82.
[24] Knopp EA, Cha S, Johnson G, et al. Glial neoplasms: dynamic contrast-enhanced T2*-weighted MR imaging. Radiology 1999;211:791–8.
[25] Dean BL, Drayer BP, Bird CR, et al. Gliomas: classification with MR imaging. Radiology 1990;174:411–5.
[26] Watanabe M, Tanaka R, Takeda N. Magnetic resonance imaging and histopathology of cerebral gliomas. Neuroradiology 1992;34:463–9.
[27] Kondziolka D, Lunsford LD, Martinez AJ. Unreliability of contemporary neurodiagnostic imaging in evaluating suspected adult supratentorial (low-grade) astrocytoma. J Neurosurg 1993;79:533–6.
[28] Sugahara T, Korogi Y, Kochi M, et al. Correlation of MR imaging determined cerebral blood volume maps with histologic and angiographic determination of vascularity of gliomas. AJR Am J Roentgenol 1998;171:1479–86.
[29] Aronen HJ, Gazit IE, Louis DN, et al. Cerebral blood volume maps of gliomas: comparison with tumor grade and histologic findings. Radiology 1994;191:41–51.
[30] McKnight TR, Noworolski SM, Vigneron DB, et al. An automated technique for the quantitative assessment of 3D-MRSI data from patients with glioma. J Magn Reson Imaging 2001;13:167–77.
[31] Kaminogo M, Ishimaru H, Morikawa M, et al. Diagnostic potential of short echo time MR spectroscopy of gliomas with single-voxel and point-resolved spatially localised proton spectroscopy of brain. Neuroradiology 2001;43:353–63.
[32] Tedeschi G, Lundbom N, Raman R, et al. Increased choline signal coinciding with malignant degeneration of cerebral gliomas: a serial proton magnetic resonance spectroscopy imaging study. J Neurosurg 1997;87:516–24.
[33] Daumas-Duport C, Scheithauer B, O'Fallon J, et al. Grading of astrocytomas: a simple and reproducible method. Cancer 1988;62: 2152–65.
[34] Noguchi T, Yoshiura T, Hiwatashi A, et al. Perfusion imaging of brain tumors using arterial spin-labeling: correlation with histopathologic vascular density. AJNR Am J Neuroradiol 2008;29:688–93.
[35] Jackson A, Kassner A, Annesley-Williams D, et al. Abnormalities in the recirculation phase of contrast agent bolus passage in cerebral gliomas: comparison with relative blood volume and tumor grade. AJNR Am J Neuroradiol 2002;23:7–14.
[36] Covarrubias DJ, Rosen BR, Lev MH. Dynamic magnetic resonance perfusion imaging of brain tumors. Oncologist 2004;9:528–37.
[37] Schaefer PW. Applications of DWI in clinical neurology. J Neurol Sci 2001;186(suppl 1):S25–35.
[38] Teng K, Zhang ZH, Jiang LL. The application of apparent diffusion coefficient in preoperative grading of gliomas. J Med Imaging 2007; 17:1250–1.
[39] Cremer D, Kraka E. Chemical bonds without bonding electron density—does the difference electron-density analysis suffice for a description of the chemical bond? Angew Chem Int Ed Engl 1984;23:627–8.
[40] Callis PR. Electronic states and luminescence of nucleic acid systems. Annu Rev Phys Chem 1983;34:329–57.
[41] Matsumoto K, Jinzaki M, Tanami Y, et al. Virtual monochromatic spectral imaging with fast kilovoltage switching: improved image quality as compared with that obtained with conventional 120-kVp CT. Radiology 2011;259:257–62.
[42] Yu L, Leng S, McCollough CH. Dual-energy CT-based monochromatic imaging. AJR Am J Roentgenol 2012;199:S9–15.
[43] Johnson TR. Dual-energy CT: general principles. AJR Am J Roentgenol 2012;199:S3–8.
[44] Simons D, Kachelriess M, Schlemmer HP. Recent developments of dual-energy CT in oncology. Eur Radiol 2014;24:930–9.
[45] Japan Association on Radiological Protection in Medicine, Japan Association of Radiological Technologists, Japan Network for Research and Information on Medical Exposure, et al. Diagnostic Reference Levels Based on Latest Surveys in Japan. J-RIME report 2015.
[46] ICRPRadiological protection in medicine. ICRP Publication 105. Ann ICRP 2007;37:1–63.
[47] Louis DN, Perry A, Reifenberger G, et al. The 2016 World Health Organization classification of tumors of the central nervous system: a summary. Acta Neuropathol 2016;131:803–20.

[48] Cha S, Tihan T, Crawford F, et al. Differentiation of low-grade oligodendrogliomas from low-grade astrocytomas by using quantitative blood-volume measurements derived from dynamic susceptibility contrast-enhanced MR imaging. AJNR Am J Neuroradiol 2005;26: 266–73.

[49] Narang J, Jain R, Scarpace L, et al. Tumor vascular leakiness and blood volume estimates in oligodendrogliomas using perfusion CT: an analysis of perfusion parameters helping further characterize genetic subtypes as well as differentiate from astroglial tumors. J Neurooncol 2011; 102:287–93.